A QUANTUM MECHANICS AND MOLECULAR MECHANICS STUDY OF THE EFFECTS OF DIFFERENT SOLVENTS AND TEMPERATURES ON THE CONNECTIONS OF METHOTREXATE DERIVATIVES ANTICANCER DRUG TO NANOTUBES CARRIERS

V. KHODADADI [a], N. HASANZADEH [a*], H. YAHYAEI [b] AND A. RAYATZADEH [a]

[a]Department of Chemistry, Ahvaz Branch, Islamic Azad University, Ahvaz, Iran.
[b]Department of Chemistry, Zanjan Branch, Islamic Azad University, Zanjan, Iran.

ABSTRACT

In this study, the interactions of two effective derivatives of the methotrexate anticancer drug with Single-wall carbon nanotubes (SWNTs) and Boron nitride nanotubes (BNNTs) in the gas phase were investigated using the DFT calculations. Through the DFT method, the effects of different solvents on the interaction of methotrexate derivatives with SWNTs and BNNTs within the Onsager self-consistent reaction field (SCRF) model, as well as the effects of temperature on the stability of interactions between compounds in various solvents were studied. Thermodynamic parameters, Frontier Molecular Orbitals (FMOs) and Total Density of States (DOS) of the title compounds were also studied using theoretical calculations. Molecular properties of the structures such as the ionization potential (I), electron affinity (A), chemical hardness (η), electronic chemical potential (μ) and electrophilicity (ω) were investigated as well. SWNTs are more suitable carriers for L-MTX and BNNTs are more suitable carriers for L-FMTX. Also, the interaction of methotrexate derivatives with SWNTs and BNNTs was examined via Amber, Opls, Charmm and MM+ force fields through the molecular mechanic (MM) method. The calculations were carried out through the Monte Carlo simulation methods at different temperatures. The effects of gas phase and various solvent media with different dielectric constants (water, DMSO, methanol, ethanol, CH2Cl2 and DMF) on the interaction of methotrexate derivatives were investigated using the aforementioned force fields. The MM+ force field, which is an exclusive force field for calculations related to macromolecules, had the lowest amount of energy and featured the most stable form of connection for Methotrexate derivatives connected to SWNTs and BNNTs. The most significant finding is that with respect to both thermodynamic properties and conformer populations, the Monte Carlo and Molecular Mechanics-Quantum Mechanics results are in agreement.

Keywords: Quantum Monte Carlo (QMC), Single-wall carbon nanotubes (SWNTs), Boron nitride nanotubes (BNNTs), methotrexate derivatives anticancer drug, Solvent effect, force field.

INTRODUCTION

Carbon nanotubes (CNTs) possess extraordinary properties and are unique nano systems. In such nanotubes, carbon atoms are interconnected through covalent bonds. These nanotubes include Single-walled nanotubes (SWNTs) and Multi-walled nanotubes (MWNTs) [1-3]. SWNTs are considered as one of the most suitable items for being used in biological systems due to their appropriate size, biocompatibility, controllable properties and ability to have reversible responses compared to biochemicals. For instance, their small size allows them to easily pass through shells and biological barriers and enter cells; they have a diameter about half of that of a DNA strand [4-5]. The applications of nanotubes and their use as drug nano-carriers have received a lot of attention recently [6-7]. In particular, functional drug-containing nanotubes (drug nano-carriers) have helped develop a new generation of drugs and have opened a new chapter of treatment in medical science [8-9]. Previous studies have proved that carbon nanotubes are not inherently toxic. Therefore, these nanotubes can be suitable options for being used as carrier nanotubes and in drug delivery [10-11].

The Boron nitride nanotube (BNNT) is a Boron compound. It is a white solid with a layered structure that resembles Graphite. In the boron-nitride structure, the strong B-N ionic bond and the covalent bond are formed simultaneously along two adjacent boron nitride nanotube layers, creating the folded single structure [12]. Nanostructures, especially boron nitride (BN) nanostructures, have great potentials for applications in pharmaceutics, medicine and industry [13-15]. BNNTs possess high elastic and tensile strength and high resistance to oxidation in air at high temperatures; they also withstand deformations more efficiently [16-17]. In Addition, BNNTs have been found to be good insulators with a large band gap (~5.5 eV) [18]. On the other hand, the thermal conductivity of BNNTs is comparable to that of CNTs, though they have better thermal stability [19]. Thus, the mechanical stiffness of BNNTs is assumed to be comparable to that of CNTs as well [20]. Furthermore, boron nitride nanotubes are non-toxic in nature compared to CNT, which makes them suitable for possible biomedical applications [21]. To minimize the toxic effects of drugs, especially anti-neoplastic drugs, drug delivery systems are used to improve cancer cell specificity of a drug during chemotherapy [22-23]. In the case of methotrexate, BNNTs are used to make the drug more water-soluble, thereby making the transportation of MTX via the bloodstream easier. Thus, there is a theory that a more water-soluble MTX-BNNT has a greater therapeutic activity [24-25]. Analysis of electrical properties including state density, charge distribution and charge transfer in the case of BNNTs containing drug molecules shows that there are changes in the molecular properties of the drug. In fact, this study attempts to help reveal more information about the experimental stages of these drugs and their interaction with BNNTs, so that they can be used experimentally.

Methotrexate (MTX) has become the most widely used second-line agent for the treatment of cancerous cells [26]. To date, MTX has been used to treat patients who have rheumatoid arthritis (RA) or other inflammatory diseases; it has also been employed to treat a number of cancers [27] and some other autoimmune diseases [28]. MTX is a folic acid analogue used as a reproduction agent. As folate receptors are over-expressed on the cell membranes of many types of cancer cells, MTX is an effective treatment for cancers [29]. Figure 1 [30] shows the working mechanism of MTX.
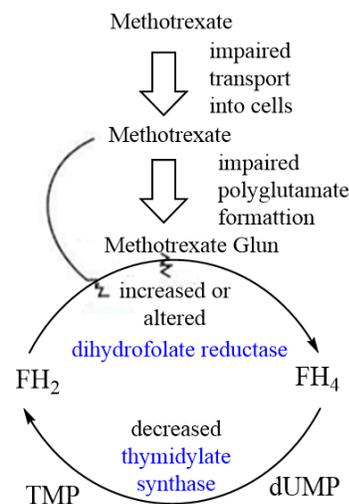
Figure 1. The mechanism of MTX drug [30].

The structure of MTX with the formula C20H22N8O5 can be seen in Figure 2. MTX is a competitive inhibitor of folic acid production [31]. Various modifications in the glutamic acid moiety have been reported with the aim of decreasing the formation rate of poly-γ-glutamates in normal cells; they include: substitution of γ-carboxyl with amide or peptide groups and replacement of glutamic acid with other amino acids; these steps have been taken with the goal

of generating a new class of antitumor agents. We prepared several MTX derivatives containing R- or γ-substituted glutamic acids [32]. The lysine and ornithine derivatives were synthesized from MTX, and both derivatives had self-same bindings [33].

Various derivatives of 2,4-diamino, N10-methylpteroyl glutamic acid (MTX) have been synthesized by modifying γ-COOH, such as MTX-N (idoacetyl) L-lysine, Cbz and NH2 groups. Moreover, some of the derivatives of MTX – such as Lysyl derivatives – have been synthesized through the reaction of γ-COOH with the amine group of lysine. These derivatives vary with respect to the number of Lysyl groups attached to them. Thus, all other derivatives exhibit less activity. The attachment of some functional groups causes changes in MTX, leading to the formation of a number of MTX derivatives [34-35]. Also, halogenated derivatives of methotrexate have been evaluated as inhibitors of human dihydrofolate reductase in cancer chemotherapy [36]. Given the wealth of attention they have received in numerous studies and their medicinal properties, the following two derivatives were used in this article (Fig 2):
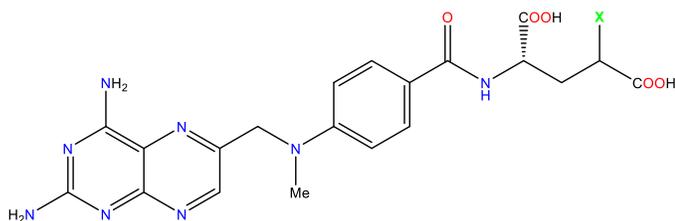
Figure 2. Chemical structure of MTX derivatives: L-MTX (1): X=H (4-(((2, 4-diaminopteridin-6-yl) methyl) (methyl) amino) benzoyl)-*L*-glutamic acid and L-FMTX (2): X=F (2S)-2- (4-(((2, 4-diaminopteridin-6-yl) methyl) (methyl) amino) benzamid)-4 -fluoropentanedioic acid.

Nowadays, designing and simulating medicine with the help of computers and specialized software have become particularly important [37]. Through this method, it is possible to save time and costs in developing new drugs by identifying the drug molecule and the receptor in the body and by using techniques that evaluate the interaction of these compounds in the same environment [38-39]. The use of computational methods plays an important role in understanding and optimization of laboratory processes that aim to evaluate the drug delivery capability of drug carriers. Computational simulation, which employs computational chemistry software used in pre-laboratory research to produce more effective drugs with less side effects, can lead to faster and more cost-effective prognosis, diagnosis and treatment in cancer patients [40-41].

In this study, structural, thermo-dynamic and electronic information for SWNTs and BNNTs with MTX derivative complexes have been presented using quantum and Monte Carlo calculations as well as molecular mechanics over a range of temperatures and solvents [42-43]. Thus, by comparing the energies computed through Monte Carlo calculations in the CHARMM, AMBER, MM+ and OPLS force fields, the differences in the complexes resulting from the incorporation of the MTX derivatives into SWNTs and BNNTs are demonstrated [44-45]. In addition to investigating the effects of interactions of MTX derivatives with SWNTs, the interactions in the gas phase as well as in the solvents DMF, DMSO, water, ethanol and methanol were also studied using different force fields and Monte Carlo calculations; the same procedure was followed for the interaction between MTX derivatives and BNNTs. The present study will help gain deeper insights about the experimental stages of these drugs and their interaction with SWNTs and BNNTs, so that they can be used experimentally.

Computational Method

In this study, the quantum chemical calculations were performed using the Gaussian 09W software [46]. The molecular structure of the title compounds in the ground state was optimized using the Density Functional Theory (DFT/B3LYP/6-31+G*) [47]. The Polarized Continuum Model (PCM) [48][47], The Frontier Molecular Orbital (FMO) analysis and electronic properties such as energies of HOMO and LUMO orbitals, HOMO-LUMO energy gap (Eg), ionization potential (I), electron affinity (A), global hardness (η), electronegativity (χ), electronic chemical potential (μ), electrophilicity (ω), and chemical softness (S) were estimated through the EHOMO and ELUMO energies using the B3LYP.6-31+G* level of theory [49-52].

The optimized molecular structures, Molecular Electrostatic Potential (MEP) maps and UV.Vis spectra were visualized using GaussView 05 program [47]. There are three types of QMC: variation, diffusion and Green's functions. These methods act with an openly correlated wave function and calculate integrals numerically, utilizing a Monte Carlo integration. These calculations are very time consuming, but they are the most accurate methods known to date. Overall, DFT calculations provide perfect and increasingly more accurate quantitative results as the molecules under consideration become smaller [53]. DFT methods are accessible in macro model programs as well. It is vital to select a level that is well-parameterized for the molecular system being investigated. Conformational interconversions are governed by precise energy parameters and geometry coordinates, which are vital in molecular systems, too. We chose the Low-energy structures found on each surface and subjected them to unrestrained quantum mechanical minimization Using B3LYP.6-31+G* SCRF [54].

Moreover, the calculations related to the interactions between MTX and Single wall carbon nanotubes (SWNTs) and Boron nitride nanotube (BNNTs) have been carried out using each of the force fields AMBER, OPLS, CHARMM and MM+ (Fig. 3 and Fig. 4). MTX derivatives are placed inside the carbon and boron-nitride nanotubes. This method is utilized in HyperChem software. Four different force fields are available in the Macro Model program. Choosing a force field that is well parameterized for the molecular system under study is very important [55-56].

The Monte Carlo method is one of the most broadly and commonly used numerical techniques, with applications in statistical physics, quantum mechanics, field theory etc [57]. With its ability to generate a canonical ensemble, Monte Carlo simulation is applied when systems have difficult integrals to be solved and should generate some random numbers to yield statistically fixed and independent values [58-59]. Due to its simplicity, a metropolis algorithm is applied more frequently than other algorithms in the Monte Carlo method [60]. Random displacement is used to determine the accuracy of the algorithm. Every move can be accepted in minor displacements; however, only a few moves are acceptable in large cases. In this study, differences in force fields are illustrated by comparing the energies calculated using force fields AMBER, OPLS, CHARMM and MM+. HyperChem professional release 7.01 is used for the Molecular Mechanics calculations. Geometry optimization as well as Monte Carlo simulation were performed using this software [11].
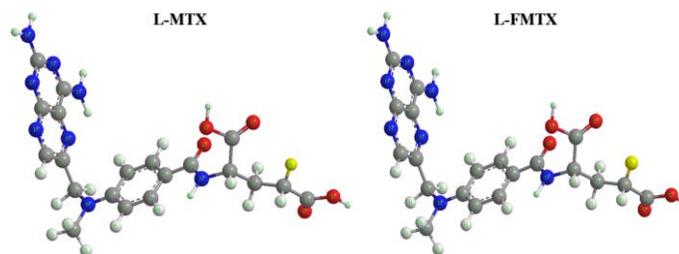
Figure 3. The theoretical geometric structure of the **L-MTX** and **L-FMTX** (optimized by B3LYP.6-31+G level).

(SWNTs)　　　　　(BNNTs)
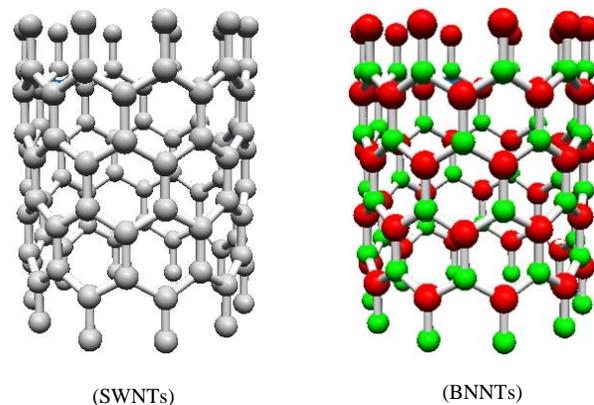
Figure 4. Single-wall carbon nanotubes (SWNTs) and Boron nitride nanotube (BNNTs) (optimized by B3LYP.6-31+G level).

RESULTS AND DISCUSSION

In macromolecules, thermodynamic parameters such as enthalpies, entropies, and free energies depend on many conformational degrees of freedom that these flexible molecules can take. The free energies of macromolecules in solutions cannot typically be estimated using Monte Carlo simulations, partially because transitions from one conformer to another occur infrequently. In addition, Molecular Mechanics simulations regularly succeed in providing more efficient samplings of conformational space in the case of macromolecules. What Monte Carlo or Molecular Dynamics simulations can achieve, however, is estimating free energy differences between similar systems. Such calculations allow, for example, comparison of binding affinities of similar drug molecules with the target receptor, thus facilitating rational design of more potent and selective drugs.

A word of caution is due here, however. Monte Carlo sampling of harmonic potentials yields classical probability distributions, while bond vibrations in the real MTX atoms with carbon nanotube molecules are quantized. Consequently, classical Monte Carlo simulations fail to precisely reproduce such thermodynamic properties as heat capacity or vibrational entropy of isolated molecules. Therefore, in this section we have used the quantum mechanics methods.

Quantum chemical methods are highly useful tools for acquiring information about molecular structures and electrochemical behaviors. A Frontier Molecular Orbitals (FMO) analysis was carried out for the compounds using the B3LYP/6-311+G (d) level [61]. FMO results such as EHOMO, ELUMO and the HOMO-LUMO energy gap (ΔE) of the title compounds have been summarized in Table 1. Table 9 presents important information regarding quantum mechanics calculations and the stability of MTX derivatives with carbon and boron-nitrite nanotubes. In this step, the L-MTX molecule was first optimized alone and then with carbon and boron-nitrite nanotubes.

The energy level of the LUMO and HOMO and their energy gaps reflect the chemical reactivity of the molecule [62]. In addition, the HOMO can act as an electron donor and the LUMO as an electron acceptor. An increased level of HOMO energy (EHOMO) for the molecule leads to a heightened ability to donate electrons to a suitable acceptor molecule that has a low-energy empty molecular orbital. E_{HOMO} and E_{LUMO} are related to ionization potential ($I=-E_{HOMO}$) and electron affinity ($A=-E_{LUMO}$), respectively [63-65]. Global hardness (η), electronegativity (χ), electronic chemical potential (μ), electrophilicity (ω) and chemical softness (S) parameters [66] are calculated using the following equations:

$$(\eta = I - A/2) \tag{1}$$

$$(\chi = I + A/2) \tag{2}$$

$$(\mu = -(I + A)/2) \tag{3}$$

$$(\omega = \mu^2/2\eta) \tag{4}$$

$$(S = 1/2\eta) \tag{5}$$

The values of these parameters are reported in Table 9. The global hardness (η) parameter is related to the energy gap (Eg = $E_{LUMO} - E_{HOMO}$) and defined as the charge transfer resistance of an atom or a group of atoms.

As shown in Table 1, the HOMO energy of the compound L-MTX with SWNTs has the lowest value (-0.29841eV). A large energy gap is indicative of high stability for the molecule. The HOMO–LUMO energy gap (ΔE) values calculated for the structures L-MTX with SWNTs and L-MTX with BNNTs are 0.15774 and 0.02094 eV, respectively. The results show that L-MTX with SWNTs is more stable. DOS plots also demonstrate the energy gaps (ΔE) calculated for the L-MTX (see Fig. 5). Table 9 shows the specifics of quantum molecular descriptors of title compounds such as electron affinity, ionization potential, electronic chemical potential, global hardness and electrophilicity. The chemical hardness (η) values for the compounds L-MTX with SWNTs and L-MTX with BNNTs are 0.07887 eV and 0.01047 eV, respectively. The L-MTX with SWNTs has the highest chemical hardness (η = 0.07887 eV); therefore, it is a hard, less reactive molecule with a wide energy gap (ΔE= 0.15774 eV).

As a form of potential energy, electronic chemical potential (μ=-(I + A)/2) has the ability to be absorbed or released during chemical reactions and might also be modified during phase transitions. The electronic chemical potential of Methotrexate with DWNTs has the largest negative value (-0.012572 eV).

Electrophilicity (ω) is a measure of energy stabilization for when the system receives an additional electronic charge from the environment. This index (ω=μ2/2η) holds information about both electron transfer (chemical potential) and stability (hardness); it also describes global chemical reactivity more precisely. The higher the value of electrophilicity index, the higher the capacity of the molecule to accept electrons. The electrophilicity index for the L-MTX with SWNTs and L-MTX with BNNTs are 0.305552 and 2.719402 eV, respectively. The L-MTX with SWNTs has the highest electrophilicity index; therefore its capacity for accepting electrons is quite high.

The dipole moment (μD) is an appropriate measure of the asymmetric nature of molecules. The composition and dimensionality of the 3D structures determine its magnitude. As shown in Table 9, all structures have a high value of dipole moment and a point group of C1, which indicates the lack of symmetry in the structures. The dipole moment for the L-MTX with SWNTs (B3LYP/6-31+G (d) =2.8907 Debye) is lower than that for L-MTX with BNNTs (9.7738 Debye, respectively). The asymmetric character of L-MTX with BNNTs is the reason behind its high dipole moment value.

As can be seen in Table 9, the HOMO energy of the compound L-FMTX with BNNTs has the lowest value (-0.29522eV). A large energy gap points to a high level of stability for the molecule. The HOMO–LUMO energy gap (ΔE) values calculated for the structures L-FMTX with SWNTs and L-MTX with BNNTs are 0.04198 and 0.15458 eV, respectively. The results show that the compound L-FMTX with BNNTs is more stable. DOS plots [43] also demonstrate the energy gaps (ΔE) calculated for the L-FMTX (Fig. 5).

Table 9 also shows the specifics of quantum molecular descriptors of title compounds, such as electron affinity, ionization potential, electronic chemical potential, global hardness and electrophilicity.

The chemical hardness (η) values for the compounds L-FMTX with SWNTs and L-FMTX with BNNTs are 0.02099 eV and 0.07729 eV, respectively. The L-FMTX with BNNTs has the highest chemical hardness (η = 0.07729 eV); therefore, it is a hard, less reactive molecule with a wide energy gap (ΔE= 0.15458 eV).

The electrophilicity index for the L-FMTX with SWNTs and L-FMTX with BNNTs is 1.575917 and 0.307242 eV, respectively. The L-FMTX with BNNTs has the highest electrophilicity index; therefore its capacity for accepting electrons is quite high. The dipole moment for the L-FMTX with SWNTs (B3LYP/6-31+G (d) =3.5689 Debye) is lower than that for the L-FMTX with BNNTs (2.6501 Debye, respectively).

As the data suggest, the amount of Gibbs free energy for L-MTX with a carbon nanotube and L-MTX with a boron-nitride nanotube is -9019.34004 Hartree and -5588.257224 Hartree, respectively. The data also indicate that the L-MTX and carbon nanotube combination has more stability. This is further confirmed by the amounts of HOMO and LUMO energies. However, the results pertaining to L-FMTX differ substantially with those related to L-MTX. The amount of Gibbs free energy for L-FMTX with a carbon nanotube and L-FMTX with a boron-nitride nanotube is -4966.985640 Hartree and -8397.302476 Hartree, respectively. The data point to the fact that the L-FMTX and boron-nitride nanotube combination has more stability, which is again confirmed by the amounts of HOMO and LUMO energies. Figure 4 shows the structures of L-MTX and L-FMTX. The two structures differ in the H and F constituents. The stability of the L-MTX and carbon nanotube combination, as well as that of the L-FMTX and boron-nitride nanotube combination is due to high electronegativity of F compared to H.

The DFT calculations have taken place in a gas phase [67-69]. The total energy of a molecule consists of the sum of translational, rotational, vibrational and electronic energies. The statistical thermochemical analysis of title compounds is carried out by placing the molecule at the room temperature of 25°C and under 1 atmospheric pressure. The thermodynamic parameters such as zero point vibrational energy, rotational constant, heat capacity (C) and entropy (S) of the title compound using the B3LYP/6-31+G (d) level are displayed in Table 1. According to this table, the values calculated for L-MTX with SWNTs are smaller than those for L-MTX with BNNTs. The results suggest that the compound L-MTX with SWNTs is more stable. However, in the case of L-FMTX, the results are different. All the thermodynamic parameters, the enthalpy, the zero-point energy and the entropy are totally in line with the changes in Gibbs free energy. According to this table, the values calculated for L-FMTX with BNNTs are smaller than those for L-FMTX with SWNTs. The results suggest that the former compound is more stable.

Table 1. The electronic properties of the Methotrexate calculated using the B3LYP/6-31+G* level of theory.

Property	L-MTX	L-MTX+ (C nanotubes)	L-MTX+ (BN nanotubes)	L-FMTX	L-FMTX+ (C nanotubes)	L-FMTX+ (BN nanotubes)
HF (Hartree)	-1569.0315828	-9020.7871662	-5589.3955307	-1666.79514	-4968.0516805	-8398.9072602
Zero-point correction(Hartree)	0.448227	1.570951	1.077289	0.436996	1.009014	1.491755
Thermal correction to Energy(Hartree)	0.478087	1.686926	1.137363	0.468411	1.065096	1.603840
Thermal correction to Enthalpy(Hartree)	0.479031	1.687870	1.138307	0.469355	1.066040	1.604784
Thermal correction to Gibbs Free Energy(Hartree)	0.383664	1.447122	1.004015	0.368044	0.937894	1.366664
Sum of electronic and zero-point Energies(Hartree)	-1568.583356	-9019.216216	-5588.318242	-1666.358144	-4967.042667	-8397.415506
Sum of electronic and thermal Energies(Hartree)	-1568.553496	-9019.100241	-5588.258168	-1666.326729	-4966.986585	-8397.303420
Sum of electronic and thermal Enthalpies(Hartree)	-1568.552552	-9019.099296	-5588.257224	-1666.325785	-4966.985640	-8397.302476
Sum of electronic and thermal Free Energies(Hartree)	**-1568.647919**	**-9019.340044**	**-5588.391516**	**-1666.427096**	**-4967.113787**	**-8397.540596**
E (Thermal) (KCal.Mol)	300.004	1058.562	713.706	293.932	668.358	1006.425
CV (Cal.Mol-Kelvi)	113.735	528.853	296.206	117.599	274.149	506.952
S (Cal.Mol-Kelvin)	200.717	506.696	282.642	213.228	269.706	501.165
Dipole moment (Debye)	10.2493	2.8907	9.7738	3.2280	0.5689	2.6501
Point Group	C1	C1	C1	C1	C1	C1
E_{HOMO} (eV)	-0.28207	-0.29841	-0.24910	-0.28577	-0.27820	-0.29522
E_{LUMO} (eV)	-0.19143	-0.14067	-0.22816	-0.19260	-0.23622	-0.14064
Eg (eV)	**0.09064**	**0.15774**	**0.02094**	**0.09317**	**0.04198**	**0.15458**
I (eV)	0.28207	0.29841	0.24910	0.28577	0.27820	0.29522
A (eV)	0.19143	0.14067	0.22816	0.1926	0.23622	0.14064
χ (eV)	0.23675	0.21954	0.23863	0.239185	0.25721	0.21793
η (eV)	0.04532	0.07887	0.01047	0.046585	0.02099	0.07729
μ (eV)	5.3121	2.8907	9.7738	1.9530	3.5689	2.6501
ω (eV)	0.618387	0.305552	2.719402	0.614033	1.575917	0.307242
S (eV)	11.03266	6.339546	47.75549	10.73307	23.82087	6.469142
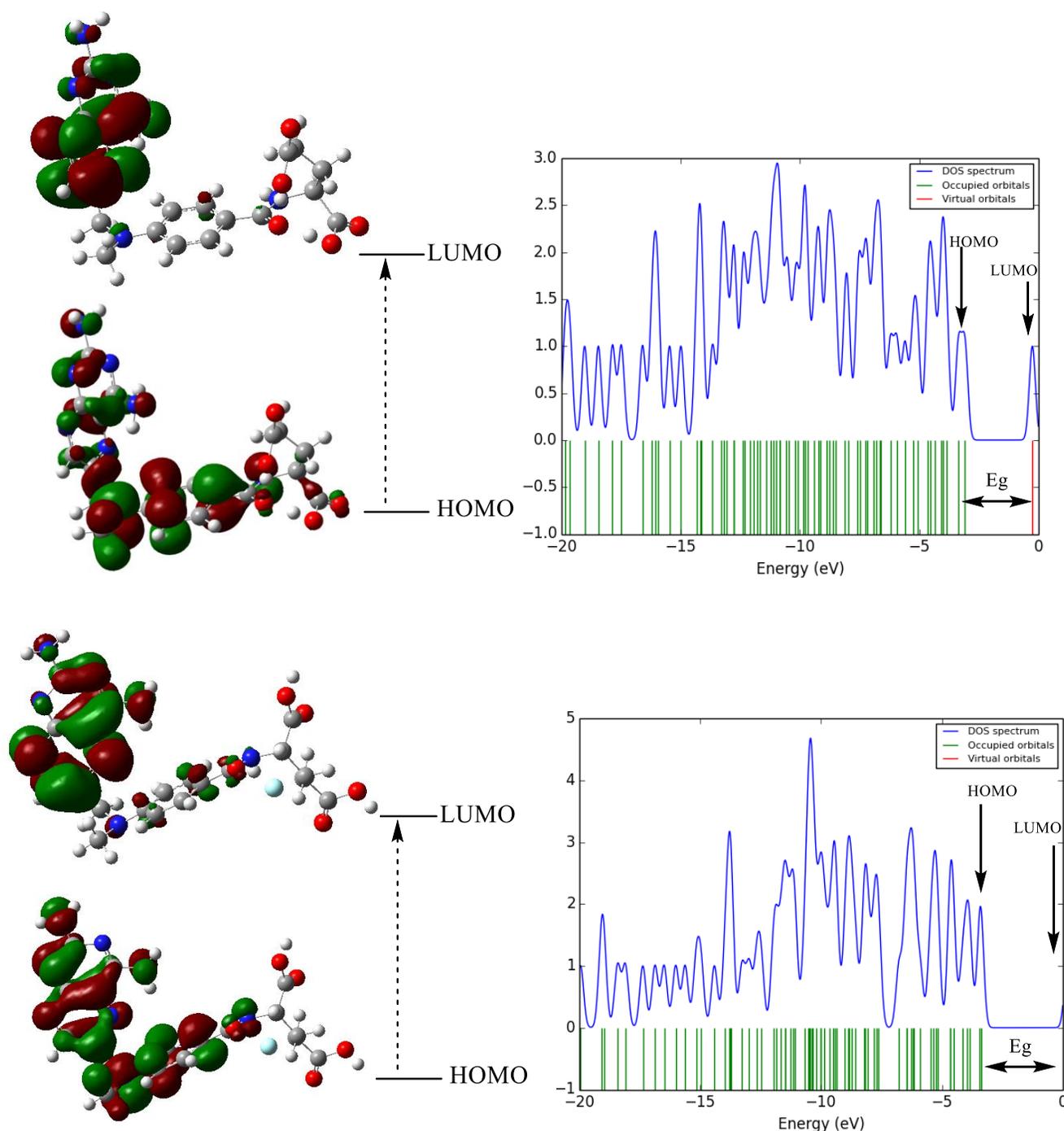
Figure 5. Calculated Frontier molecular orbitals and DOS plots of L-MTX and L-FMTX (ΔE: Energy gap between LUMO and HOMO)

In the present study, calculations related to the interaction between MTX derivatives (L-MTX and L-FMTX) and Single Wall carbon nanotubes and Boron nitride nanotubes (SWNTs & BNNTs) have been carried out using AMBER, OPLS, CHARMM (BIO+) and MM+ force fields. Biomolecules are complex systems. Their structures are represented by multidimensional rugged energy landscapes with a huge number of local minima separated by high energy barriers. Thus, any simulation study primarily deals with adequate description of the atomistic interaction or force field and convergence of the configuration space sampling of such a complex energy landscape. Efficient sampling can be achieved through enhanced conformational search techniques. The experimental values of the properties predicted by a force field are signs of its quality. There are four predominantly used force field families for molecular mechanic simulations at the time, including AMBER, OPLS, CHARMM (BIO+) and MM+. These classic force fields have constantly been improved and verified;

however, given the intricacies of the energy landscape, the successful application of these fields in many systems remains to be validated. Thus, how the employed force field affects the simulation results is a question worth investigating.

Among other appropriate tools for evaluating probability distributions are Monte Carlo algorithms. Due to their tendency to sample low energy regions of conformational spaces, Monte Carlo-based algorithms are highly useful in finding important conformations of flexible biomolecules. With small adjustments, a Monte Carlo program can calculate a histogram of a distance distribution for a particle in harmonic potential. Such histograms illustrate that at any given temperature, the L-MTX and L-FMTX (with SWNTs & BNNTs) distance adopts a range of values. It is also observed that the range of values gets broader with temperature, indicating increased amplitude of motion of atoms at higher temperatures.

The effect of different solvents and temperatures on the L-MTX and L-FMTX (with SWNTs & BNNTs) were studied through quantum mechanics calculations and molecular mechanic simulation. Differences in force fields were illustrated by comparing the energies calculated using AMBER, OPLS, CHARM (Bio+) and MM+ force fields. Using this method, The Total (E tot), Potential (E pot) and Kinetic (E kin) energies (kcal/mol) were calculated for the Native structure through Monte Carlo simulation in different solvents and in AMBER, OPLS, CHARMM(Bio+) and MM+ force fields. The results have been listed in tables 2 to 9.

Fig. 6-9 show the E Kin changes (kcal/mol) calculated versus temperature at different dielectric constants (water (ε = 78.39), DMSO (ε = 46.8), methanol (ε = 32.63), ethanol (ε = 24.55), CH2Cl2 (ε = 8.93) and DMF (ε = 39.8)) through Monte Carlo simulation in the four force fields (AMBER, OPLS, CHARMM (Bio+) and MM+). The results of Monte Carlo calculations (tables 2-5 & charts 6-11) indicate that in the gas phase and while in the Amber force field, L-MTX and L-FMTX connected to SWNTs and BNNTs are the most stable and have the lowest amount of energy. The methanol solvent displayed the lowest amount of energy and proved to be the most stable solvent for the simulation, when L-MTX connected to SWNTs was simulated in water, DMSO, methanol, ethanol, CH2Cl2 and DMF solvents.

Similar results have been reported for OPLS and CHARMM force fields. The calculations related to the MM+ force field produced a notable result though. In this field, water was the most stable and the most suitable among the aforementioned solvents for simulation, since it had the lowest amount of energy. No doubt this was positively related to the dielectric constant of the solvents. Water had the highest dielectric constant; therefore, it is considered to be the most suitable solvent for L-MTX connected to SWNTs.

Substances with a high dielectric constant are easily polarized. Polarization allows countercharges to be placed around an ion, resulting in Coulombic interactions between the solvent and the ion, which in turn promote solubilization of the ion through competing with interionic interactions. In a similar vein, a polar solvent – one with a high dielectric constant – will form stabilizing interactions with the solute that compete with solute-solute interactions, thereby solubilizing polar molecules. The dielectric constant of the solvent also affects the interactions in the solution that involve ions and polar molecules; as the dielectric constant increases, the intermolecular energy is reduced.

It is noteworthy that tables 6-9 and charts 12-17, which display the results for L-FMTX connected to BNNTs, show that the results are highly consistent with those related to L-MTX connected to SWNTs; in the force fields Amber, OPLS and CHARMM, methanol is the most stable solvent and in the MM+ field, water is the most stable solvent.

On the other hand, water is a biological solvent and acts as the main foundation for chemical reactions. Results of chemical calculations can be influenced by solvation, which can push the simulation conditions toward the most stable form. However, the results for L-FMTX connected to BNNTs are very significant, since they are highly consistent with the behavior of SWNTs and point to methanol and water as being the most efficient solvents for this simulation. Given that performing calculations for Molecular Mechanics force fields requires selecting an appropriate force field in the beginning, the specifications of these 4 fields were closely investigated. Our choice was guided by force field equation for these fields.

Finally, we found that the MM+, which is an exclusive force field for calculations related to macromolecules, had the lowest amount of energy and featured the most stable form of connection for Methotrexate derivatives connected to SWNTs and BNNTs. Notably, in some solvents and at certain temperatures, the CHARMM force field demonstrates a similar behavior and puts our compound in a stable situation. However, since electrostatic reactions are calculated through bipolar junctions by using point charges in the MM+ field, the field managed to simulate our desired system in the most optimal way. Therefore, the MM+ was chosen as the most efficient force field. It should further be noted that the results of Quantum Mechanics calculations are also consistent with the current findings; SWNTs are more suitable carriers for L-MTX and BNNTs are more suitable carriers for L-FMTX. The results of Monte Carlo, Molecular Mechanics and Quantum Mechanics calculations have been justified.

Table 2. The Total (E tot), Potential (E pot) and Kinetic (E kin) energies (kcal/mol) calculated for the Native structure through Monte Carlo simulation in different solvents in the Amber force field (L-MTX)

Monte Carlo.Amber											
Temperature		**298K**	**300K**	**302K**	**304K**	**306K**	**308K**	**310K**	**312K**	**314K**	**316K**
Gas (ε r =1)	E kin	369.5223	372.0023	374.4823	376.9623	379.4423	381.9223	384.4024	386.8824	389.3624	391.8424
	E pot	1215035	94875.69	18072.93	4770.186	1891.809	977.8239	596.4858	386.4485	288.5021	230.005
	E tot	1215405	95247.69	18447.41	5147.148	2271.251	1359.746	980.8882	773.3309	677.8645	621.8474
Water (ε r =78.39)	E kin	1632.649	1643.606	1654.564	1665.521	1676.478	1687.436	1698.393	1709.35	1720.308	1731.265
	E pot	1107903	100680.9	27634.59	14565.76	10818.86	9247.115	8228.382	7479.221	7042.025	6654.092
	E tot	1109536	102324.5	29289.16	16231.28	12495.34	10934.55	9926.775	9188.571	8762.333	8385.357
Methanol (ε r =32.63)	E kin	636.0047	640.2732	644.5416	648.8101	653.0786	657.3471	661.6156	665.8841	670.1526	674.4211
	E pot	1245003	114642.2	24691.49	7086.969	2992.702	1800.709	1247.194	913.8457	695.4784	575.4344
	E tot	1245639	115282.4	25336.04	7735.779	3645.78	2458.056	1908.81	1579.73	1365.631	1249.855
Ethanol (ε r =24.55)	E kin	769.2459	774.4086	779.5713	784.734	789.8968	795.0595	800.2222	805.3849	810.5477	815.7104
	E pot	1203230	108701.5	22846.09	6582.576	2828.231	1709.052	1221.028	1001.106	880.3172	732.2387
	E tot	1203999	109475.9	23625.66	7367.31	3618.128	2504.111	2021.251	1806.491	1690.865	1547.949
DMSO (ε r =46.8)	E kin	813.6596	819.1204	824.5812	830.042	835.5028	840.9636	846.4244	851.8852	857.346	862.8068
	E pot	1342842	144844.7	35076.15	10938.13	4311.248	2199.194	1498.577	1100.033	949.6149	810.0334
	E tot	1363655	145663.8	35900.73	11768.18	5146.751	3040.157	2345.001	1951.918	1806.961	1672.84
DMF (ε r =38.3)	E kin	881.1685	887.0824	892.9962	898.9101	904.824	910.7379	916.6518	922.5657	928.4795	934.3934
	E pot	1553272	168777.7	45394.16	16272.58	7950.383	4364.089	2774.878	2017.792	1619.377	1274.044
	E tot	1554153	169664.8	46287.15	17171.49	8855.207	5274.826	3691.53	2940.358	2547.856	2208.438

Table 3. The Total (E tot), Potential (E pot) and Kinetic (E kin) energies (kcal/mol) calculated for the Native structure through Monte Carlo simulation in different solvents in the Opls force field (L-MTX with SWNTs)

Monte Carlo. Opls											
Temperature		**298K**	**300K**	**302K**	**304K**	**306K**	**308K**	**310K**	**312K**	**314K**	**316K**
Gas (ε_r =1)	E kin	369.5223	372.0023	374.4823	376.9623	379.4423	381.9223	384.4024	386.8824	389.3624	391.8424
	E pot	1772265	166731.1	33535.61	8798.063	3279.649	1805.931	1152.415	863.3952	674.8464	541.0597
	E tot	1772634	167103.1	33910.09	9175.026	3659.091	2187.853	1536.817	1250.278	1064.209	932.9021
Water (ε_r =78.39)	E kin	1632.649	1643.606	1654.564	1665.521	1676.478	1687.436	1698.393	1709.35	1720.308	1731.265
	E pot	2083885	183886.4	63832.85	38714.33	30203.93	25987.91	23566.26	21998.69	20839.26	19754.51
	E tot	2085518	185530	65487.41	40379.85	31880.41	27675.35	25264.65	23708.04	22559.56	21485.77
Methanol (ε_r =32.63)	E kin	636.0047	640.2732	644.5416	648.8101	653.0786	657.3471	661.6156	665.8841	670.1526	674.4211
	E pot	2110145	198664.3	43810.95	12732.32	5276.441	3001.545	2092.551	1575.327	1280.798	1130.354
	E tot	2110781	199304.5	44455.49	13381.13	5929.52	3658.892	2754.166	2241.211	1950.951	1804.775
Ethanol (ε_r =24.55)	E kin	76902459	774.4086	779.5713	784.734	789.8968	795.0595	800.2222	805.3849	810.5477	815.7104
	E pot	2073174	158448.3	40652.37	11500.14	4368.956	2650.884	1725.141	1380.603	1140.458	958.1391
	E tot	2073943	186222.7	41431.95	12284.88	5158.853	3355.943	2525.363	2185.985	1951.005	1773.849
DMSO (εr =46.8)	E kin	813.6569	819.1204	824.5812	830.042	835.5028	840.9636	846.4244	851.8852	857.3460	862.8068
	E pot	2309454	226424.08	55216.16	15722.95	5772.276	3009.73	2037.231	1583.689	1262.06	1093.549
	E tot	2310268	227243.9	56040.75	16553	6607.258	3850.693	2883.626	2435.574	2119.406	1656.356
DMF (εr =38.3)	E kin	881.1685	877.0824	892.9956	898.9102	904.824	910.7379	916.6518	992.5657	928.4795	934.3943
	E pot	2373464	273300.9	76129.45	27600.37	12226.23	6033.796	3608.733	2427.096	1844.653	1498.755
	E tot	2374346	274188	77022.45	28499.28	13130.84	6944.534	4525.385	3349.662	2773.132	2433.148

Table 4. The Total (E tot), Potential (E pot) and Kinetic (E kin) energies (kcal/mol) calculated for the Native structure through Monte Carlo simulation in different solvents in the CHARMM force field (L-MTX with SWNTs)

Monte Carlo.Charmm											
Temperature		**298K**	**300K**	**302K**	**304K**	**306K**	**308K**	**310K**	**312K**	**314K**	**316K**
Gas (ε_r =1)	E kin	369.5223	372.0023	374.4823	376.9623	379.4423	381.9223	384.4024	386.8824	389.3624	391.8424
	E pot	571579.5	49052.96	9449.037	2750.36	1361.871	856.5552	599.3778	446.3805	343.2243	305.3477
	E tot	571949	49424.96	9823.35	3127.323	1741.313	1238.478	983.7802	833.2629	732.5867	697.1901
Water (ε_r =78.39)	E kin	1632.649	1643.606	1654.564	1665.521	1676.478	1687.436	1698.393	1709.35	1720.308	1731.265
	E pot	618115.4	51317.69	11306.14	4102.412	1577.696	374.0644	-329.8485	-867.5709	-1247.758	-1462.535
	E tot	619748	52961.3	12960.71	5767.933	3254.175	2061.5	1368.545	841.7796	472.5496	268.7304
Methanol (ε_r =32.63)	E kin	636.0047	640.2732	644.5416	648.8101	653.0786	657.3471	661.6156	665.8841	670.1526	674.4211
	E pot	662941.2	61217.51	13531.14	4606.004	2491.551	1617.565	1223.629	981.8296	825.4841	703.4496
	E tot	663577.2	61857.79	14175.68	5254.814	3144.63	2274.912	1885.244	1647.714	1495.637	1377.871
Ethanol (ε_r =24.55)	E kin	769.2459	774.4086	779.5713	784.734	789.8968	795.0595	800.2222	805.3849	810.5477	815.7104
	E pot	662354.4	62431.12	13415.3	4372.998	2223.693	1486.936	1229.257	946.9232	800.0959	731.11
	E tot	663123.6	63205.52	14194.87	5157.732	3013.59	2281.996	1929.479	1752.308	1610.644	1546.82
DMSO (εr =46.8)	E kin	813.6596	819.1204	824.5812	830.042	835.5028	840.9636	846.4244	851.8852	857.346	862.8068
	E pot	766294.3	87140.02	21484.24	6906.317	2941.12	1886.499	1399.431	1104.159	995.512	872.8668
	E tot	767108	87959.25	22309.25	7736.25	3776.2356	2727.325	2445.885	1956.044	1853.858	1735.675
DMF (εr =38.3)	E kin	881.1685	877.0824	892.9625	898.2581	904.4578	910.7379	916.2587	922.5686	928.2587	934.2101
	E pot	905576	123315.01	33588.02	12112.03	5937.56	3511.025	2533.64	1958.25	1578.25	1374.045
	E tot	906457.2	124202.01	34481.02	13011.25	6862.02	4421.0258	3450.025	2881.258	2507.25	2308.258

Table 5. The Total (E tot), Potential (E pot) and Kinetic (E kin) energies (kcal/mol) calculated for the Native structure through Monte Carlo simulation in different solvents in the MM+ force field (L-MTX with SWNTs)

						Monte Carlo.MM+					
Temperature		**298K**	**300K**	**302K**	**304K**	**306K**	**308K**	**310K**	**312K**	**314K**	**316K**
Gas (ε_r =1)	E kin	369.5223	372.0023	374.4823	376.9623	379.4423	381.9223	384.4024	386.8824	389.3624	391.8424
	E pot	54285.77	15756.75	6110.059	3043.559	1810.011	1215.896	898.1151	688.2434	553.4915	427.8488
	E tot	54655.3	16128.75	6484.541	3420.521	2189.453	1597.818	1282.517	1075.126	942.8539	819.6912
Water (ε_r =78.39)	E kin	1632.258	1643.025	1654.890	1665.028	1676.981	1687.987	1698.214	1709.351	1720.921	1731.324
	E pot	246270.3	19302.25	154461.1	128223.04	111018.25	97520.36	84963.25	73770.63	63986.02	55082.36
	E tot	247903.12	194664.02	156116.31	129889.65	112695.23	99207.23	86661.23	75480.23	65706.21	56813.25
Methanol (ε_r =32.63)	E kin	636.0047	640.2732	644.5416	648.8101	653.0786	657.3471	661.6156	665.8841	670.1526	674.4211
	E pot	264320.2	209363.2	168875.6	142200.6	123731.7	109095.1	96174.95	84833.81	74129.24	64710.34
	E tot	264956.2	210003.5	169520.2	142849.5	124384.8	109752.4	96836.56	85499.69	74799.4	65384.76
Ethanol (ε_r =24.55)	E kin	769.2546	774.4086	779.5713	784.734	789.2587	795.0595	800.2222	805.2347	810.7123	815.2174
	E pot	251251.1	200183.9	161017.9	134599.7	117273.3	103198.2	89837.1	78091.2	67984.2	59233.2
	E tot	252020.4	200958.3	161797.4	135384.4	118063.2	103993.6	90637.21	78896.21	68795.20	60049.25
DMSO (ε r =46.8)	E kin	813.6596	819.1204	824.5812	830.042	835.5028	840.9636	846.4244	851.8852	875.346	862.8068
	E pot	273355.4	218738.4	177119	148530.1	129651.9	113657.7	100138.7	87823.95	77045.2	67538.76
	E tot	274169.1	219557.5	177943.6	149360.1	130487.4	114498.6	100928.1	88675.84	77902.55	68401.57
DMF (ε r =38.3)	E kin	881.1685	877.0824	892.9962	898.9101	904.824	910.7379	916.6518	922.5657	928.4795	934.3934
	E pot	334050.6	226510.2	217634.9	183354.2	160342.7	142128.2	125601.4	110880.8	97296.04	85741.55
	E tot	334931.8	267397.2	218527.9	184253.1	161247.5	143038.9	126518.1	111803.3	98224.52	86675.94
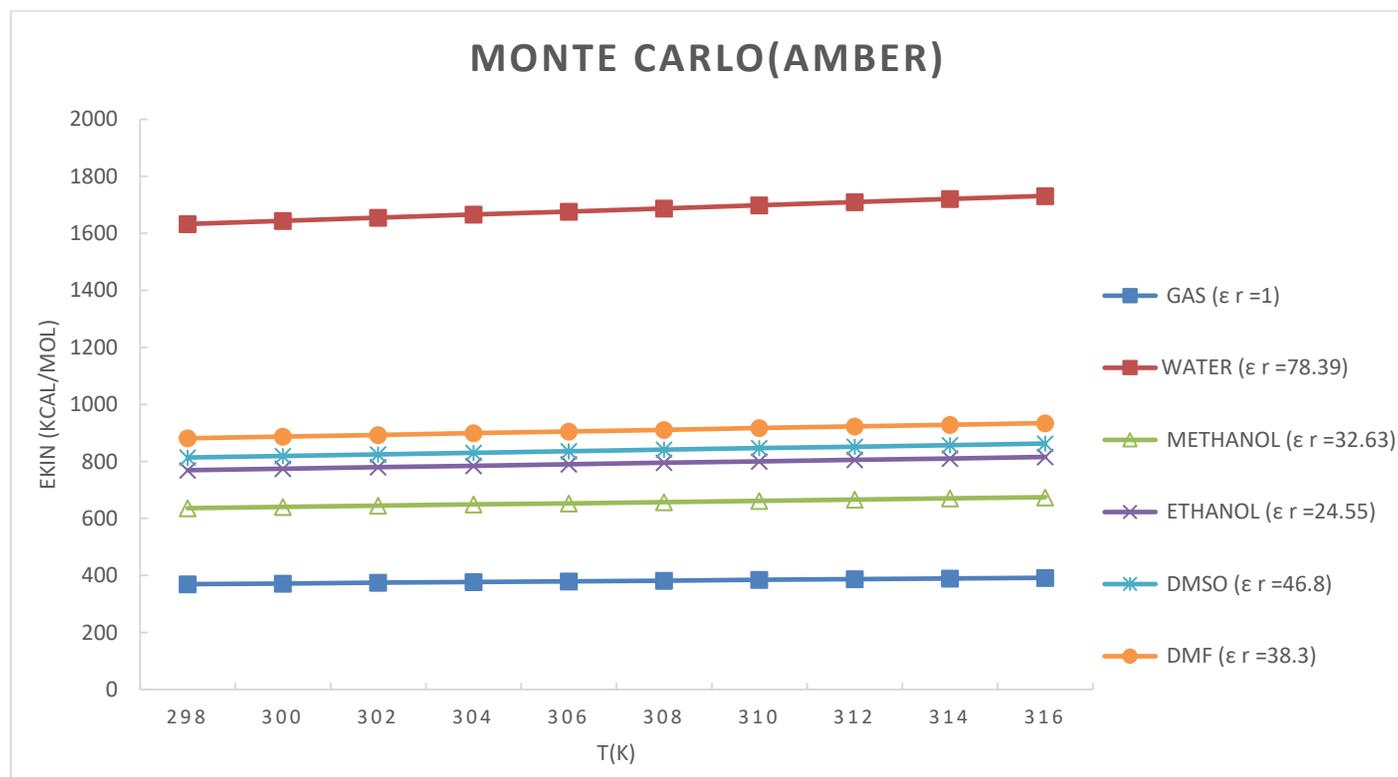
Figure 6. EKin changes (kcal.mol) calculated versus temperature at different dielectric constants through Monte Carlo simulation in the Amber force field for L-MTX with SWNTs.
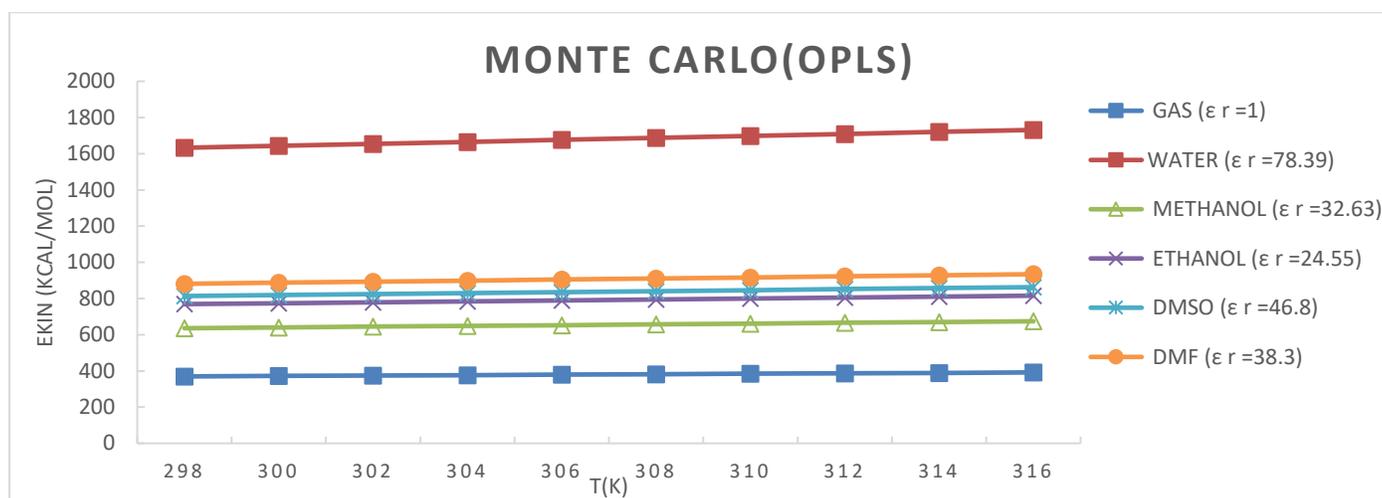
Figure 7. EKin changes (kcal.mol) calculated versus temperature at different dielectric constants through Monte Carlo simulation in the OPLS force field for L-MTX with SWNTs.
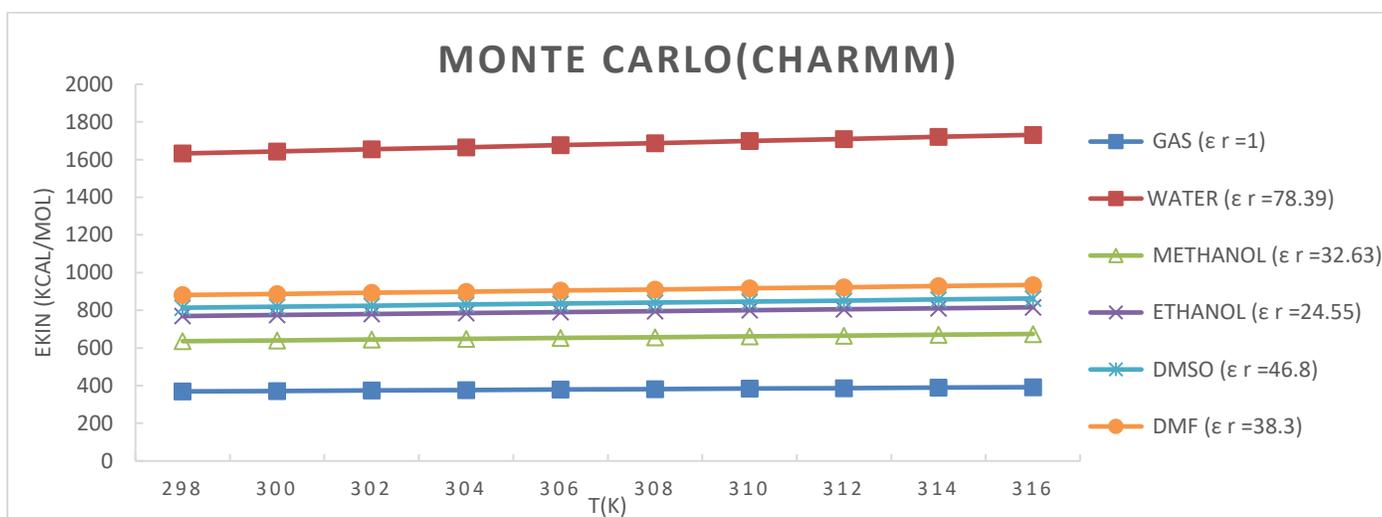
Figure 8. EKin changes (kcal.mol) calculated versus temperature at different dielectric constants through Monte Carlo simulation in the CHARMM force field for L-MTX with SWNTs.
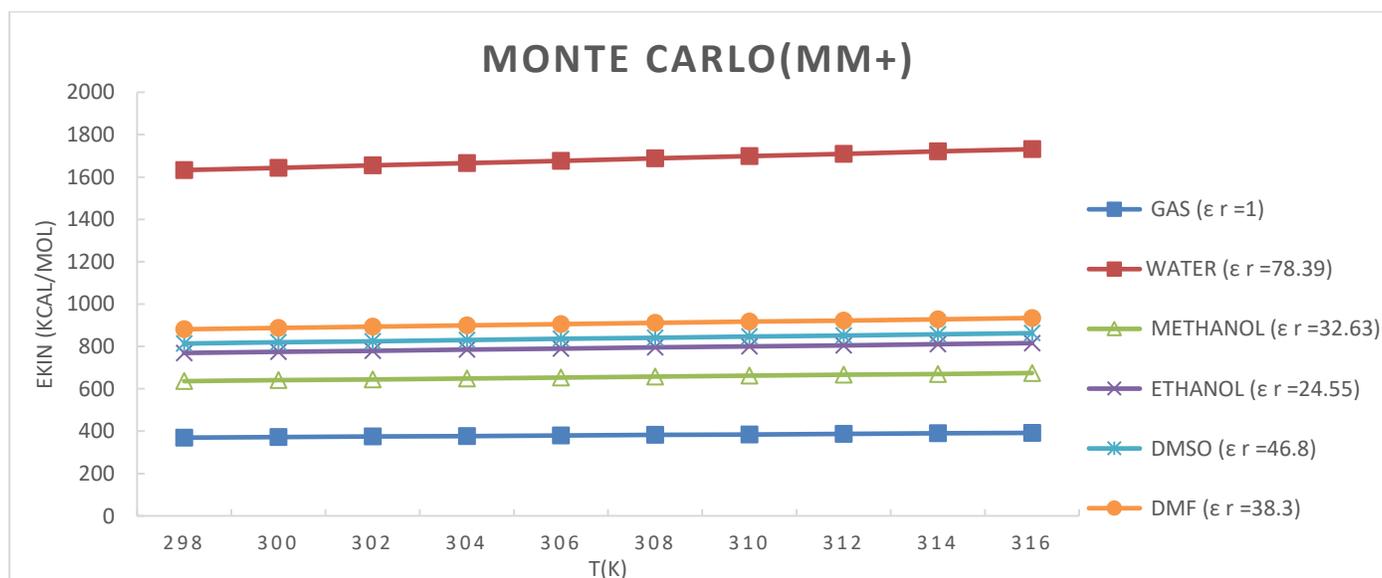
Figure 9. EKin changes (kcal.mol) calculated versus temperature at different dielectric constants through Monte Carlo simulation in the MM+ force field for L-MTX with SWNTs.
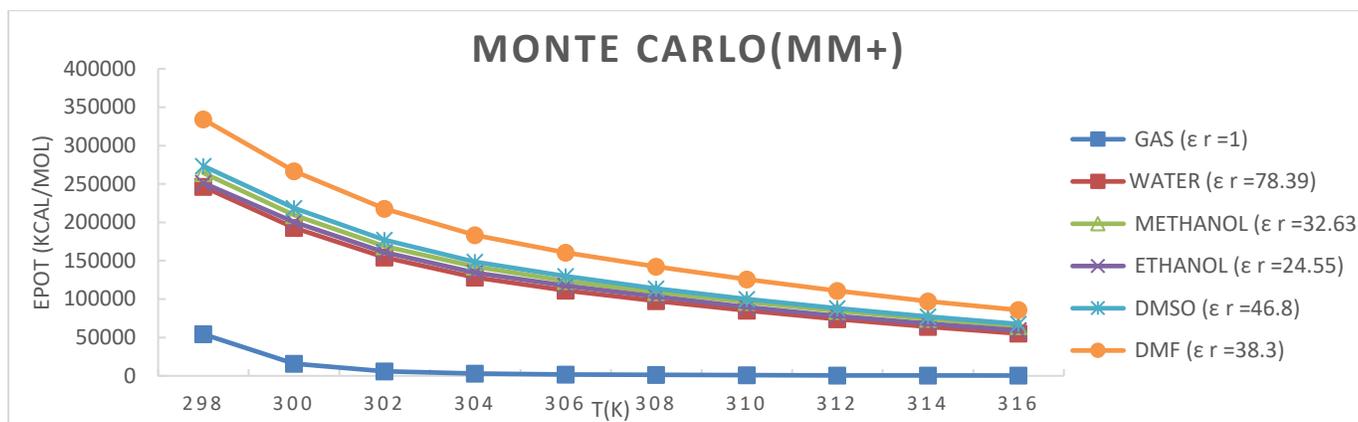
Figure 10. EPot changes (kcal.mol) calculated versus temperature at different dielectric constants through Monte Carlo simulation in the MM+ force field for L-MTX with SWNTs.
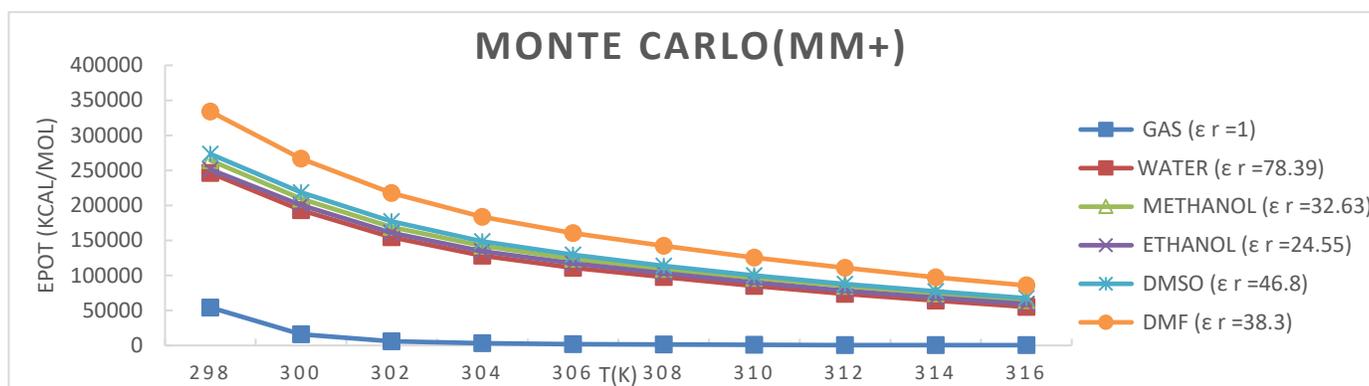
Figure 11. ETot changes (kcal.mol) calculated versus temperature at different dielectric constants through Monte Carlo simulation in the MM+ force field for L-MTX with SWNTs.

Table 6. The Total (E tot), Potential (E pot) and Kinetic (E kin) energies (kcal/mol) calculated for the Native structure through Monte Carlo simulation in different solvents in the Amber force field (L-FMTX with BNNTs)

Monte Carlo.Amber											
Temperature		**298K**	**300K**	**302K**	**304K**	**306K**	**308K**	**310K**	**312K**	**314K**	**316K**
Gas ($\varepsilon_r =1$)	E kin	369.5223	372.0023	374.4823	376.9623	379.4423	381.9223	384.4024	386.8824	389.3624	391.8424
	E pot	1142735	94865.64	18303.79	4647.02	1834.974	972.0237	587.2981	394.5939	304.2547	197.403
	E tot	1143104	95237.64	18678.27	5023.982	2214.416	1353.946	971.7005	781.4763	693.6171	589.2454
Water ($\varepsilon_r =78.39$)	E kin	1629.984	1640.924	1651.863	1662.803	1673.742	1684.681	1695.621	1706.56	1717.5	1728.439
	E pot	1096642	98711.55	26880.44	14338.82	10659.22	8864.739	7781.433	7141.914	6658.069	6314.386
	E tot	1098272	100352.5	28532.3	16001.62	12332.96	10549.42	9477.054	8848.474	8375.569	8042.826
Metanol ($\varepsilon_r =32.63$)	E kin	636.0047	640.2732	644.5416	648.8101	653.0786	657.3471	661.6156	665.8841	670.1526	674.4211
	E pot	1279321	130933	30253.88	9665.178	4374.126	2548.176	1680.624	1166.651	980.7566	715.7875
	E tot	1279957	131573.2	30898.42	10313.99	5027.205	3205.523	2342.239	1832.535	1650.909	1390.209
Ethanol ($\varepsilon_r =24.55$)	E kin	777.2403	782.4567	787.6731	792.8895	798.1059	803.3222	808.5386	813.755	818.9714	824.1878
	E pot	1270246	107898	21995.52	6122.308	2672.688	1585.394	1153.461	858.065	773.4414	659.9271
	E tot	1271023	108680.4	22783.19	6915.198	3470.794	2388.716	1961.999	1671.82	1592.413	1484.115
DMSO ($\varepsilon_r =46.8$)	E kin	813.6596	819.1204	824.5812	830.042	835.5028	840.9636	846.4244	851.8852	857.346	862.8068
	E pot	1359596	135193.8	30189.1	8644.713	3741.646	2148.814	1426.887	1093.304	870.8363	763.3856
	E tot	1360409	136012.9	31013.68	9474.755	4577.149	2989.778	2273.311	1945.189	1728.182	1626.192
DMF ($\varepsilon_r =38.3$)	E kin	881.1685	887.0824	892.9962	898.9101	904.824	910.7379	916.6518	922.5657	928.4795	934.3934
	E pot	1275730	114925.9	24774.87	6946.043	2883.357	1708.11	1200.27	1013.348	833.981	721.7818
	E tot	1276611	115812.9	25667.87	7844.953	3789.182	2618.848	2116.922	1935.913	1762.461	1656.265

Table 7. The Total (E tot), Potential (E pot) and Kinetic (E kin) energies (kcal/mol) calculated for the Native structure through Monte Carlo simulation in different solvents in the OPLS force field (L-FMTX with BNNTs)

Monte Carlo.OPLS											
Temperature		**298K**	**300K**	**302K**	**304K**	**306K**	**308K**	**310K**	**312K**	**314K**	**316K**
Gas (ε r =1)	E kin	369.5223	372.0023	374.4823	376.9623	379.4423	381.9223	384.4024	386.8824	389.3624	391.8424
	E pot	1965648	164206.9	33649.14	9358.676	3457.705	1769.1	1158.373	830.4087	633.6891	496.2554
	E tot	1966017	164578.9	34023.62	9735.639	3837.147	2151.023	1542.775	1217.291	1023.051	888.0978
Water (ε r =78.39)	E kin	1629.984	1640.924	1651.863	1662.803	1673.742	1684.681	1695.621	1706.56	1717.5	1728.439
	E pot	2094370	198506	64325.85	38926.22	30434.71	25968.6	23209.8	21298.77	19912.09	18889.24
	E tot	2096000	200146.9	65977.72	40589.02	32108.45	27653.28	24905.42	23005.33	21629.59	20617.68
Methanol (ε r =32.63)	E kin	636.0047	640.2732	644.5416	648.8101	653.0786	657.3471	661.6156	665.8841	670.1526	674.4211
	E pot	2343471	230921.9	55124.66	16652.99	7053.134	3920.395	2570.881	1883.181	1517.791	1280.233
	E tot	2344107	231562.2	55769.2	17301.81	7706.213	4577.742	3232.497	2549.065	2187.944	1954.654
Ethanol (ε r =24.55)	E kin	777.2403	782.4567	787.6731	792.8895	798.1059	803.3222	808.5386	813.755	818.9714	824.1878
	E pot	2889709	269417.9	68568.48	19707.84	7369.325	3870.296	2523.986	1833.309	1468.068	1183.452
	E tot	2890486	270200.4	69536.15	20500.73	8167.431	4673.618	3332.525	2647.064	2287.039	2007.639
DMSO (ε r =46.8)	E kin	813.6596	819.1204	824.5812	830.042	835.5028	840.9636	846.4244	851.8852	857.346	862.8068
	E pot	2373698	216770.4	51601.83	15087.13	5974.574	3397.155	2180.909	1619.642	1383.075	1182.843
	E tot	2374511	217589.5	52624.41	15917.17	6810.076	4238.119	3027.333	2543.527	2240.421	2045.65
DMF (ε r =38.3)	E kin	881.1685	887.0824	892.9962	898.9101	904.824	910.7379	916.6518	922.5657	928.4795	934.3934
	E pot	2203015	197073	42786.12	12371.11	4913.181	2722.508	1873.174	1428.213	1210.222	1059.561
	E tot	2203896	197960	43679.11	13270.02	5818.005	3633.264	2789.826	2350.779	2138.702	1993.995

Table 8. The Total (E tot), Potential (E pot) and Kinetic (E kin) energies (kcal/mol) calculated for the Native structure through Monte Carlo Simulation in different solvents in the CHARMM force field (L-FMTX with BNNTs)

Monte Carlo.Charmm											
Temperature		**298K**	**300K**	**302K**	**304K**	**306K**	**308K**	**310K**	**312K**	**314K**	**316K**
Gas (ε r =1)	E kin	369.5223	372.0023	374.4823	376.9623	379.4423	381.9223	384.4024	386.8824	389.3624	391.8424
	E pot	586516.9	49778.8	9861.559	2957.149	1391.578	797.6654	524.1795	419.3601	349.0755	263.6077
	E tot	586886.4	50150.8	10236.04	3334.111	1771.02	1179.588	908.5819	806.2425	738.4379	655.4501
Water (ε r =78.39)	E kin	1629.984	1640.924	1651.863	1662.803	1673.742	1684.681	1695.621	1706.56	1717.5	1728.439
	E pot	580286	50015.74	10822.28	4045.975	1632.549	376.2494	-408.6071	-919.0168	-1278.327	-1530.636
	E tot	581915.9	51656.67	12474.14	5708.778	3306.291	2060.931	1287.014	787.5437	439.1726	197.8038
Methanol (ε r =32.63)	E kin	636.0047	640.2732	644.5416	648.8101	653.0786	657.3471	661.6156	665.8841	670.1526	674.4211
	E pot	738310.8	81171.33	20200.17	6862.643	3291.717	1956.663	1432.668	1085.132	907.6039	743.0048
	E tot	738946.8	81811.6	20844.71	7511.453	3944.796	2614.01	2094.284	1751.016	1577.756	1417.426
Ethanol (ε r =24.55)	E kin	777.2403	782.4567	787.6731	792.8895	798.1059	803.3222	808.5368	813.755	818.9714	824.1878
	E pot	986643.3	126666.6	32740.86	10776.3	5001.039	3054.866	2249.027	1675.546	1369.627	1228.446
	E tot	987420.5	127449.1	33528.53	11569.19	5799.144	3858.189	3057.566	2489.301	2188.559	2052.633
DMSO (ε r =46.8)	E kin	813.6596	819.1204	824.5812	830.42	835.5028	840.9636	864.4244	851.8552	857.346	862.8068
	E pot	716422.8	79379.78	17109.43	5419.058	2856.074	1866.675	1355.04	1162.605	1011.852	880.7916
	E tot	717236.4	80196.9	17934.01	6249.1	3691.577	2707.639	2201.465	2014.49	1869.198	1743.598
DMF (ε r =38.3)	E kin	881.1685	887.0824	892.9262	898.9101	904.824	910.7379	916.6518	922.5657	928.4795	934.3934
	E pot	660813.8	64232.28	13891.77	4512.75	2467.091	1727.232	1401.041	1251.961	1184.178	1069.467
	E tot	661694.9	65119.36	14784.77	5411.66	3371.915	2637.97	2317.693	2174.527	2112.657	2003.86

Table 9. The Total (E tot), Potential (E pot) and Kinetic (E kin) energies (kcal/mol) calculated for the Native structure through Monte Carlo simulation in different solvents in the MM+ force field (L-FMTX with BNNTs)

Temperature		298K	300K	302K	304K	306K	308K	310K	312K	314K	316K
Gas (ε r =1)	E kin	191.8673	193.155	194.4427	195.7304	197.0181	198.3058	199.5935	200.8812	202.1689	203.4566
	E pot	1479.404	655.6518	492.8714	489.8405	470.9847	460.0471	461.0492	424.7249	432.992	441.904
	E tot	1671.271	848.8069	687.3142	685.5709	668.0028	658.3529	660.6427	625.6061	635.161	645.3607
Water (ε r =78.39)	E kin	1561.587	1572.067	1582.548	1593.028	197.0181	1613.989	1624.47	1634.95	1645.43	1655.911
	E pot	18688.64	11972.32	7590.633	5262.345	4107.78	3259.293	2599.388	2179.092	1811.395	1571.224
	E tot	2025.33	13544.38	9173.18	7055.374	5711.289	4873.282	4223.585	3814.043	3456.828	3227.134
Methanol (ε r =32.63)	E kin	458.3497	461.4259	464.5021	467.5783	470.6544	473.7306	476.8068	479.8829	482.9591	486.0353
	E pot	40507.78	29290.68	22471.8	17951.32	14028.16	11554.74	9531.721	8179.061	7063.156	6388.415
	E tot	40966.13	29752.11	22936.3	18418.89	14498.81	12028.47	10008.53	8658.944	7546.115	6874.451
Ethanol (ε r =24.55)	E kin	591.5909	595.5613	599.5318	603.5022	607.4726	611.443	615.4134	619.3838	623.3542	627.3246
	E pot	32385.32	24101.97	18567.27	14918.58	12081.58	10105.09	8474.525	7332.273	6389.992	5672.525
	E tot	32976.92	24697.53	19166.81	15522.08	12689.06	10716.53	9089.938	7951.657	7013.349	6292.859
DMSO (ε r =46.8)	E kin	636.0047	640.2732	644.5416	648.8101	653.0776	657.3471	661.6156	665.8841	670.1526	674.4211
	E pot	278379.1	221019.9	185756.2	158494.7	137388.8	121422	108744.2	98028.74	88391.26	80790.44
	E tot	279015.1	221660.1	186400.7	159143.5	138041.9	122079.4	109405.8	98694.23	89061.41	81464.86
DMF (ε r =38.3)	E kin	724.8321	729.6968	734.5614	739.4261	744.2907	749.1554	754.02	758.8847	763.7493	768.6139
	E pot	67352.25	50109.04	39000.96	31635.91	26596.85	22678.25	19522.2	17139.19	15221.89	13700.51
	E tot	68077.08	50838.73	39735.52	32375.33	27340.93	23427.44	20276.22	17898.07	15985.64	14469.13

The header row spanning all solvent-rows reads "Monte Carlo.MM+".
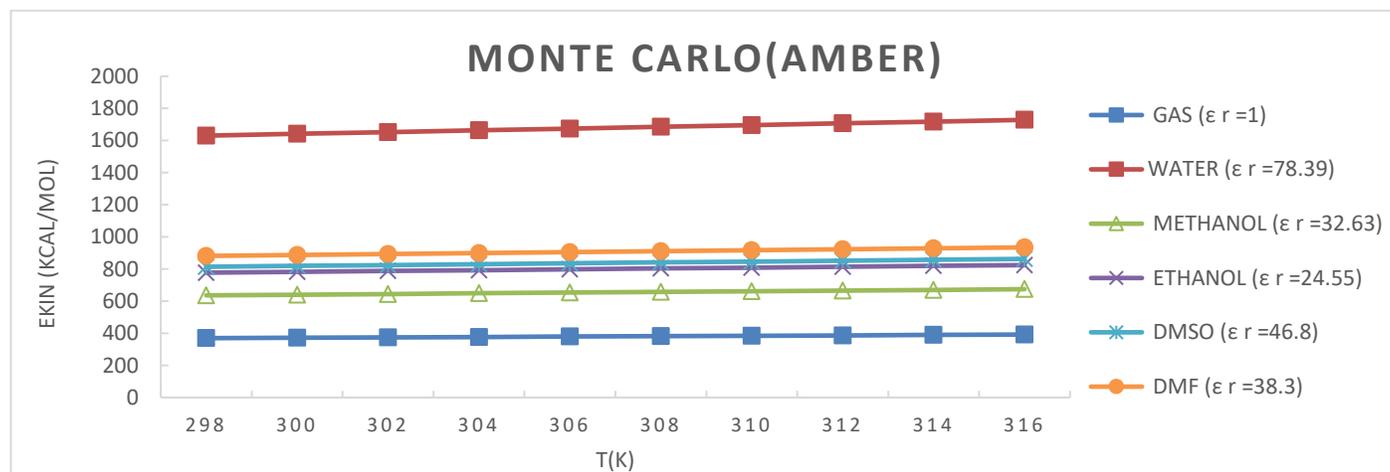
Figure 12. EKin changes (kcal.mol) calculated versus temperature at different dielectric constants through Monte Carlo simulation in the Amber force field for L-FMTX with BNNTs.
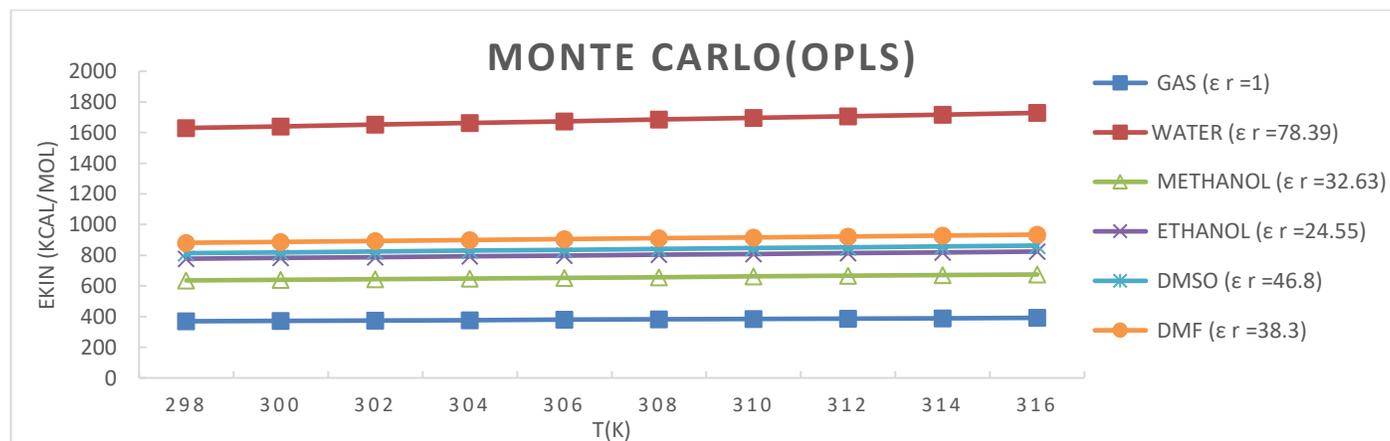
Figure 13. EKin changes (kcal.mol) calculated versus temperature at different dielectric constants through Monte Carlo simulation in the OPLS force field for L-FMTX with BNNTs.
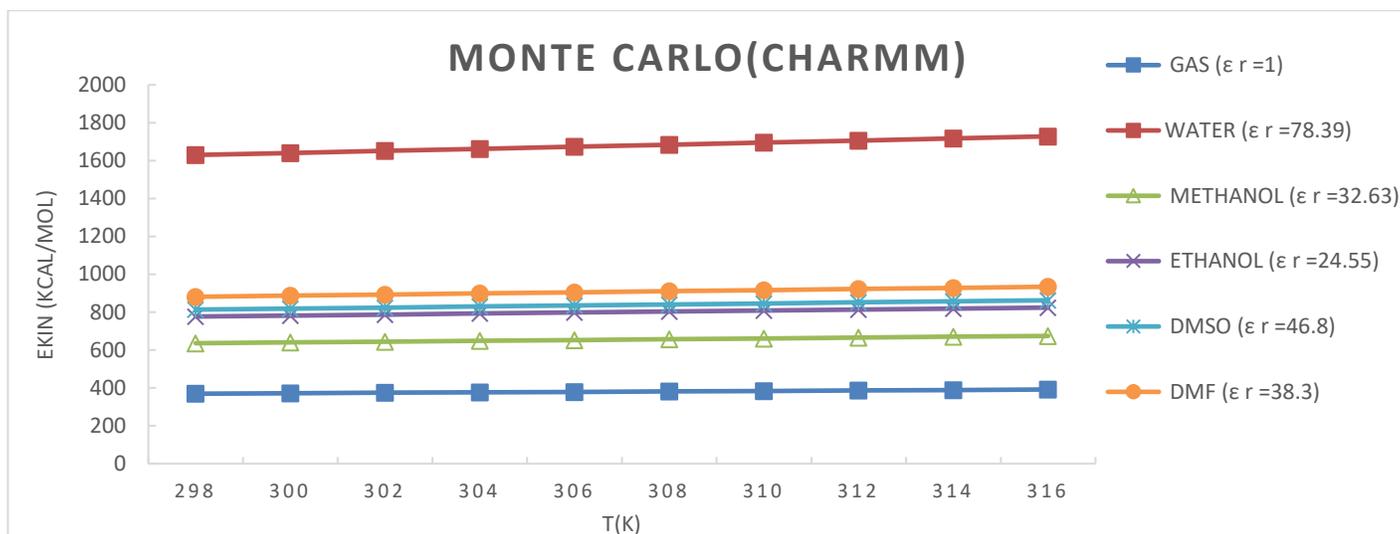
Figure 14. EKin changes (kcal.mol) calculated versus temperature at different dielectric constants through Monte Carlo simulation in the CHARMM force field for L-FMTX with BNNTs.
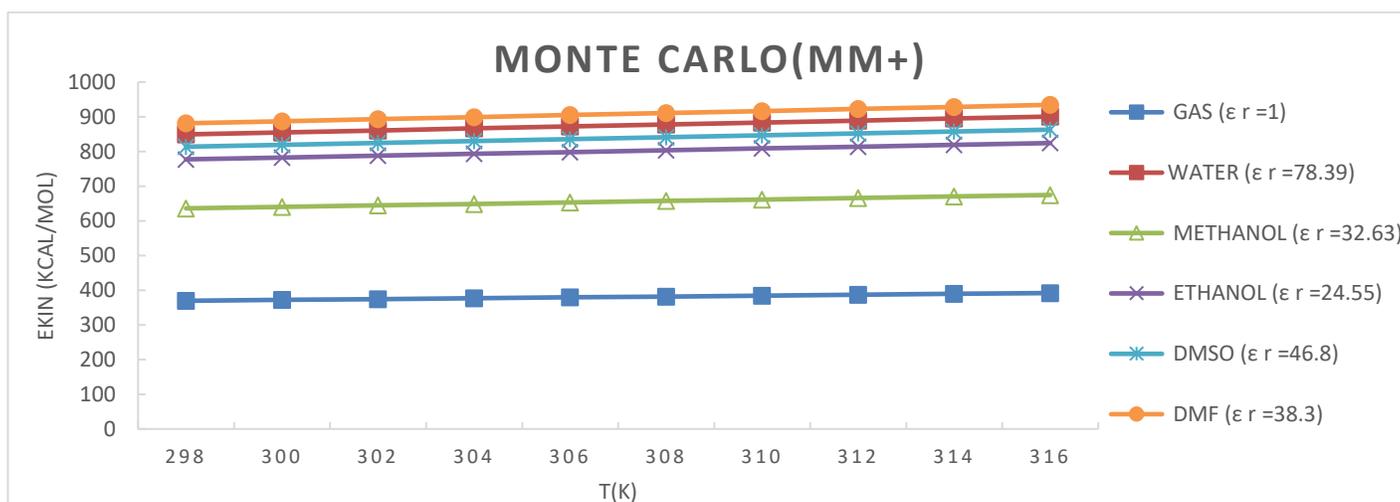
Figure 15. EKin changes (kcal.mol) calculated versus temperature at different dielectric constants through Monte Carlo simulation in the MM+ force field for L-FMTX with BNNTs.
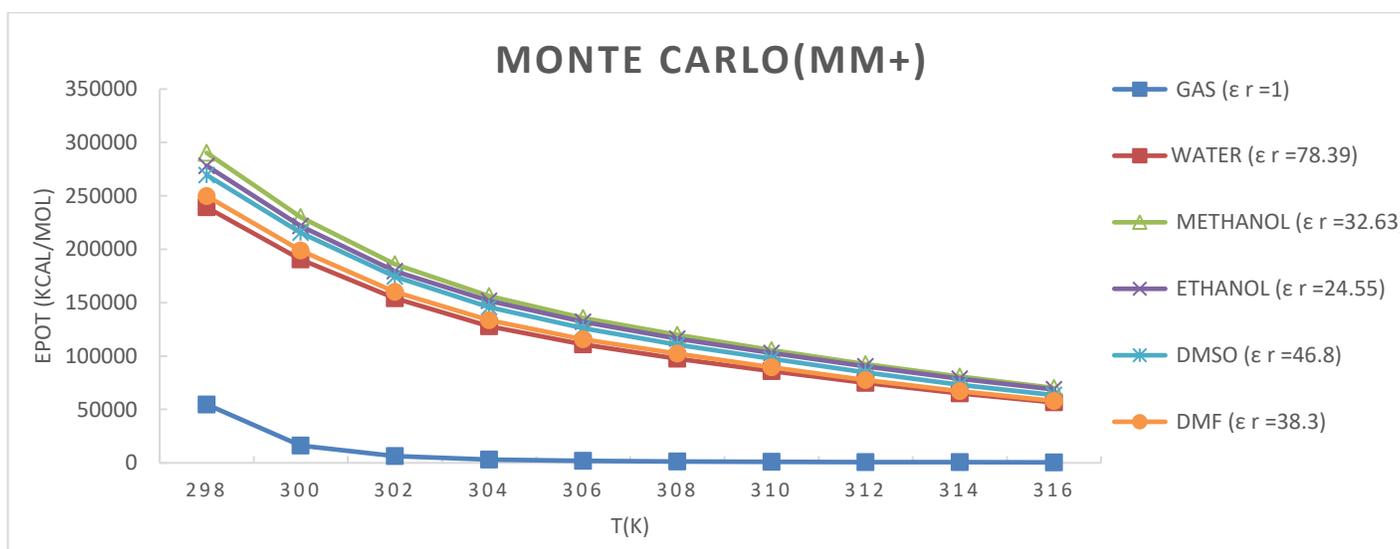
Figure 16. EPot changes (kcal.mol) calculated versus temperature at different dielectric constants through Monte Carlo simulation in the MM+ force field for L-FMTX with BNNTs.
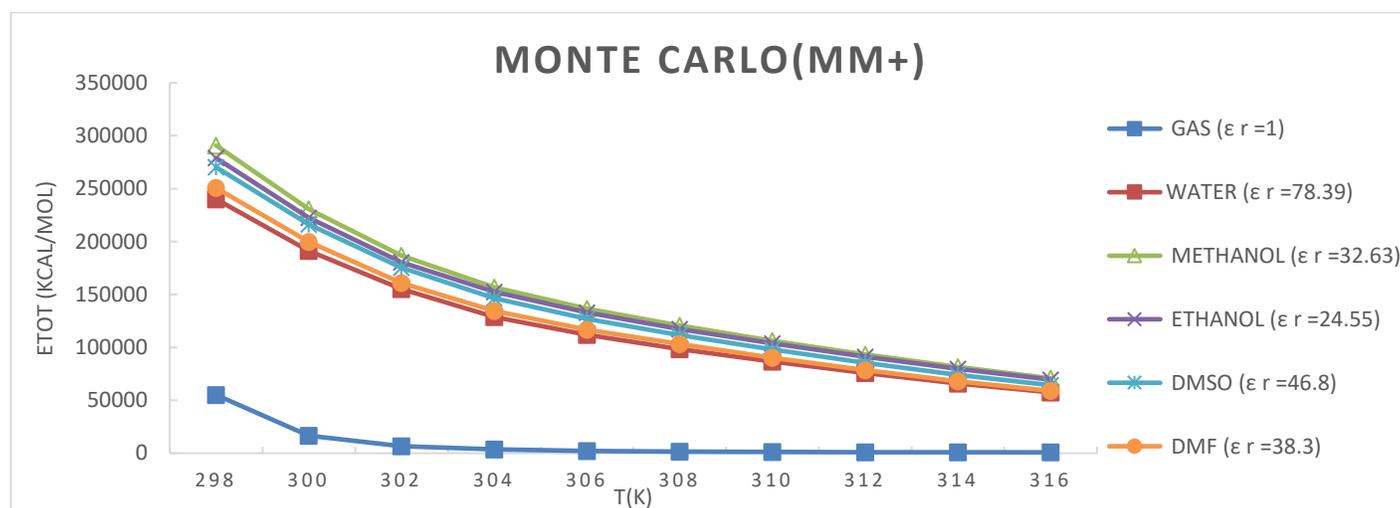
Figure 17. ETot changes (kcal.mol) calculated versus temperature at different dielectric constants through Monte Carlo simulation in the MM+ force field for L-FMTX with BNNTs.

CONCLUSION

In this study, the interaction of two effective derivatives of the anticancer drug methotrexate with Single-wall carbon nanotubes (SWNTs) and Boron nitride nanotubes (BNNTs) in the gas phase has been investigated using the DFT calculations. Through the DFT method, we studied the effects of different solvents on the interaction of methotrexate derivatives with SWNTs and BNNTs within the Onsager self-consistent reaction field (SCRF) model; we also studied the effects of temperature on the stability of the interaction between compounds in various solvents. We resorted to theoretical calculations for investigating Total Density of States (DOS), Frontier Molecular Orbitals (FMOs) and thermodynamic parameters of the title compounds. The molecular properties of the structures such as ionization potential (I), electron affinity (A), chemical hardness (η), electronic chemical potential (μ) and electrophilicity (ω) were analysed. The data showed that the L-MTX and carbon nanotube combination had more stability. This was further confirmed by the amounts of HOMO and LUMO energies and Gibbs free energy. However, the results pertaining to L-FMTX differed substantially with those related to L-MTX.

In addition, the data pointed to the fact that the L-FMTX and boron-nitride nanotube combination had more stability, which was also confirmed by the amounts of HOMO and LUMO energies. The two structures differed in the H and F constituents. High electronegativity of F compared to H resulted in the stability of both L-MTX and carbon nanotube combination, and L-FMTX and boron-nitride nanotube combination.

The effect of different solvents and temperatures on the L-MTX and L-FMTX (with SWNTs & BNNTs) was studies through quantum mechanics calculations and molecular mechanic simulation. Differences in force fields were illustrated by comparing the energies calculated using AMBER, OPLS, CHARM (Bio+) and MM+ force fields. The methanol solvent displayed the lowest amount of energy and proved to be the most stable solvent for the simulation, when L-MTX connected to SWNTs was simulated in water, DMSO, methanol, ethanol, CH2Cl2 and DMF solvents. Similar results have been reported for OPLS and CHARMM force fields. However, the calculations related to the MM+ force field yielded a notable result. In the MM+ field, water was the most stable and the most suitable among the aforementioned solvents for simulation, since it had the lowest amount of energy. This was certainly positively related to the dielectric constant of the solvents. Water had the highest dielectric constant; therefore, it was considered to be the most suitable solvent for L-MTX connected to SWNTs.

It is noteworthy that the results for L-FMTX connected to BNNTs were highly consistent with those related to L-MTX connected to SWNTs; in the force fields Amber, OPLS and CHARMM, methanol was the most stable solvent and in the MM+ field, water was the most stable solvent. Finally, we found that the MM+, which is an exclusive force field for calculations related to macromolecules had the lowest amount of energy and featured the most stable form of connection for Methotrexate derivatives connected to SWNTs and BNNTs. Notably, in some

solvents and at certain temperatures, the CHARMM force field demonstrated a similar behaviour and put our compound in a stable situation. However, since electrostatic reactions are calculated through bipolar junctions by using point charges in the MM+ field, the field managed to simulate our desired system in the most optimal way. Therefore, the MM+ force field was chosen as the most efficient field.

It should further be noted that the results of Quantum Mechanics calculations are also consistent with the current findings; SWNTs are more suitable carriers for L-MTX and BNNTs are more suitable carriers for L-FMTX. The results of Monte Carlo, Molecular Mechanics and Quantum Mechanics calculations are thus justified.

Delivering anti-cancer drugs through SWNTs and BNNTs is a considerable breakthrough in the field of nanotechnology. Conventional management of cancer with chemotherapeutic agents can have adverse effects on healthy tissues. Thus, development of CNTs -based efficient drug delivery systems is imperative for delivering anti-cancer drugs. Even though nano-technology is fairly developed, it is still far from clinical applications due to several challenges. However, SWCNTs- and BNNTs-based drug delivery systems are promising approaches for delivering anti-cancer drugs to targeted organs or tissues. The observations and results of this review paper indicated that SWNTs- and BNNTs-based drug delivery systems might be highly effective and able to provide adequate scientific data for clinical support.

REFERENCES

1. X. Li, Y. Peng, X. Qu, *Nucleic Acids Research*. 34, 3670, (**2006**)
2. C. Klumpp, K. Kostarelos, M. Prato, A. Bianco, *Biochimica et Biophysica Acta (BBA) - Biomembranes*. **1758**, 404, (2006)
3. N. Sinha, J. T. W. Yeow, *IEEE transitions on nanobioscience*. **4**, 180, (2005)
4. N. Nishiyama, K. Kataoka, *Pharmacology & therapeutics*. **112**, 630, (2006)
5. H. Mizusako, T. Tagami, K. Hattori, T. Ozeki, *Journal of pharmaceutical sciences*. **104**, 2934 (2015)
6. Q. He, J. Shi, *Jurnal of Materials Chemistry*. **21**, 5845, (2011)
7. G. Kwon, S. Suwa, M. Yokoyama, T. Okano, Y. Sakurai, K. Kataoka, *Journal of Controlled Release*. **29**, 17, (1994)
8. A. Mahmud, X. B. Xiong, H. M. Aliabadi, A. Lavasanifar, Journal *of Drug Targeting*. **15**, 553 (2007)
9. S. Khatri, N. G. Das, S. K. Das, *Journal of pharmacy & bioallied sciences*. **6**, 297, (2014)
10. J. E. Kim, J. Y. Shin, M. H. Cho, *Archives of Toxicology*. **86**, 685, (2012)
11. C. Sun, J. S. Lee, M. Zhang, *Advanced drug delivery reviews*. **60**, 1252, (2008)

12. R. Arenal, A. Lopez-Bezanilla, *Computational Molecular Science*. **5**, 299, (2015)

13. G. Ciofani, *Expert opinion on drug delivery.* **7**, 889, (2010)

14. J. H. Kim, T.V. Pham, J. H. Hwang, C. S. Kim, M. J. Kim, *Nano convergence*. **5**, 1, (2018)

15. J. Iqbal, K. Ayub, *Journal of Alloys and Compounds*. **687**, 976, (2016)

16. D. Golberg, X. D. Bai, M. Mitome, C. C. Tang, C. Y. Zhi, Y. Bando, *Acta materialia*. **55**, 1293, (2007)

17. D. Lahiri, F. Rouzaud, T. Richard, A. K. Keshri, S. R. Bakshi, L. Kos, A. Agarwal, *Acta biomaterialia*. **6**, 3524, (2010)

18. W. An, C. H. Turner, *the Journal of Physical Chemistry Letters*. **1**, 2269, (2010)

19. C. W. Chang, W. Q. Han, A. Zettl, *Journal of Vacuum Science & Technology B: Microelectronics and Nanometer Structures Processing, Measurement, and Phenomena*. **23**, 1883, (2005)

20. T. He, T. Li, A. Huang, Z. Tang, X. Guan, *Physica E: Low-dimensional Systems and Nanostructures*. **107**, 182, (2019)

21. G. Ciofani, S. Danti, G. G. Genchi, B. Mazzolai, V. Mattoli, *biocompatibility and potential spill-over in nanomedicine. Small.* **9**, 1672, (2013)

22. Z. Khatti, S. M. Hashemianzadeh, *European Journal of Pharmaceutical Sciences.* **88**, 291, (2016)

23. F. Azarakhshi, M. Sheikhi, S. Shahab, M. Khaleghian, K. Sirotsina, H. Yurlevich, D. Novik, *Chemical Papers*. **75**, 1521, (2021)

24. Z. Mahdavifar, R. Moridzadeh, *Journal of Inclusion Phenomena and Macrocyclic Chemistry*. **79**, 443, (2014)

25. P. N. Samanta, K. K. Das, *RSC advances*. **6**, 92547, (2016)

26. B. N. Cronstein, *Arthritis & Rheumatism*. **39**, 1951, (1996)

27. M. Wojtoniszak, K. Urbas, M. Peruzyńska, M. Kurzawski, M. Droździk, E. Mijowska, *Chemical Physics Letters.* **568**, 151, (2013)

28. H. Matsuoka, N. Ohi, M. Mihara, H. Suzuki, K. Miyamoto, N. Maruyama, T. Kuroki, *Journal of medicinal chemistry.* **40**, 105, (1997)

29. T. M. Goszczyński, B, Filip-Psurska, K. Kempińska, J. Wietrzyk, J. Boratyński, *Pharmacology research & perspectives.* **2**, e00047, (2014)

30. R. Segal, M. Yaron, B. Tartakovsky, *arthritis and rheumatism*. **20**, 190, (1990)

31. J. A. Moura, C. J. Valduga, E. R. Tavares, I. F. Kretzer, D. A. Maria, R. C. Maranhão, *journal of nanomedicine*. **6**, 2285, (2011)

32. S. Moura, J. Noro, P. Cerqueira, C. Silva, A. Cavaco-Paulo, A. Loureiro, *International journal of pharmaceutics*. **575**, 118924, (2020)

33. R. J. Kempton, A. M. Black, G. M. Anstead, A. A. Kumar, d. T. Blankenship, J. H. Freisheim, *Journal of medicinal chemistry*. **25**, 475-(1982)

34. A. Nemat, I. N. Khan, S. Kalsoom, S. A. Malik, S. Ayub, F. Adnan, M. A. Kamal, M. Iqbal, *Journal of Biomolecular Structure and Dynamics*. **38**, 1, (2020)

35. Y. Kokuryo, K. Kawata, T. Nakatani, A. Kugimiya, Y. Tamura, K. Kawada, M. Ohtani, *Journal of medicinal chemistry*. **40**, 3280, (1997)

36. N. Uddin, S. Ahmed, A. M. Khan, M. Mazharol Hoque, M. A. Halim, *Journal of Biomolecular Structure and Dynamics*. **38**, 901, (2020).

37. S. Ekins, J. Mestres, B. Testa, *British Journal of Pharmacology*. **152**, 21, (2007)

38. L. Fraenkel, W. B. Nowell, G. Michel, C. Wiedmeyer. *Annals of the Rheumatic Diseases*. **77**, 678, (2018)

39. A. L. Mathews, A. Coleska, P. B. Burns, K. C. Chung, *Arthritis Care & Research*. **68**, 318, (2016)

40. P. Workman, *Cold Spring Harbor Symposia on Quantitative Biology*. **70**, 499, (2005)

41. I. Collins, P. Workman, *Nature Chemical Biology*. **2**, 689, (2006)

42. A. D. MacKerell, D. Bashford, M. Bellott, et al, *J. Phys. Chem. B. 102*, 3586, (1998)

43. A. D. MacKerell Jr, M. Feig, *Journal of Computational Chemistry*. **25**, 1400, (2004)

44. W. L. Jorgensen, D. S. Maxwell, J. Tirado-Rives, *J. Am. Chem. Soc.* **118**, 11225, (1996)

45. V. Hornak, R. Abel, A Okur, B. Strockbine, A. Roitberg, C. Simmerling, *Proteins*. **65**, 712, (2006)

46. M. J. Frisch, G. W. Trucks, H. B. Schlegel, et al, Gaussian 09 revision A02, Gaussian, Inc., Wallingford CT, (2009)

47. A. Frisch, A. B. Nielson, A. J. Holder, **2000**, GAUSSVIEW User Manual, Gaussian Inc.; Pittsburgh, PA.

48. A. D.J. Becke, *Chem. Phys. 98*, 5648, (1993)

49. J. Tomasi, B. Mennucci, R. Cammi, *Chem. Rev*. **105**, 2999, (2005)

50. S. Shahab, M. Sheikhi, L. Filippovich, E. Dikusar, H. Yahyaei, R. Kumar, M. Khaleghian, *J. Mol. Struct*. **1157**, 536, (2018)

51. H. Yahyaei, S. Sharifi, S. Shahab, M. Sheikhi. M. Ahmadianarog, *Letters in Organic Chemistry.* **18**, 115, (2021)

52. S. Shahab, M. Sheikhi, L. Filippovich, R. Kumar, E. Dikusar, H. Yahyaei, M. Khaleghian, *Journal of Molecular Structure*. **1148**, 134, (2017)

53. [53] A. Szczepanska, J. L. Espartero, A. Moreno-Vargas, A. T. Carmona, I. Robina, S. Remmert, C. Parish, *J. Org. Chem.* **72**, 6776, (2007)

54. N. Metropolis, A. W. Rosenbluth, M. N. Rosenbluth, A. H. Teller, E. Teller, *J. Chem. Phys*. **21**, 1087, (2004)

55. HyperChem 7.0. (2001) Hypecube Inc., FL. Gainesville,

56. H. Yahyaei, M. Monajjemi, H. Aghaie, K. Zare, *Journal of Computational and Theoretical Nanoscience*. **10**, 2332, (2013)

57. M. Kastner, *Communications in Nonlinear Science and Numerical Simulation*. **15**, 1589, (2010)

58. W. K. Hastings, *Biometrika*. **57**, 97, (1970)

59. J. S. Liu, F. Liang, W. H. Wong, *Journal of the American Statistical Association*. **95**, 121, (2000)

60. J. A. Champion, S. Mitragotri, *Natl Aead Sei.* **103**, 4930, (2006)

61. SL. Kinnings, N. Liu, N. Buchmeier, P. J. Tonge, L. Xie, P. E. Bourne, *PLOS Computational Biology*. **5**, e1000423, (2009)

62. I. Collins, P. Workman, *Nature Chemical Biology.* **2**, 689, (2006)

63. N. Scheinfeld, *Dermatology online journal*. **12**, 15, (2006)

64. BN. Cronstein, *Pharmacol Rev*. **57**, 163, (2005)

65. M. R. Sawaya, J. Kraut, *Biochemistry*, **36**,586, (1997)

66. L. M. Meyer, F. R. Miller, M. J. Rowen, G. Bock, J. Rutzky, *Acta Haematologica*. **4**, 1571, (1950)

67. S. Majedi, L. Sreerama, E. Vessally, F. Behmagham, *J. Chem. Lett.* **1**, 25, (2020).

68. N. Shajari, H. Yahyaei, *physical chemistry research*, **4**, 705, (2020).

69. H. Yahyaei, S. Shahab, M. Sheikhi, et al, *Spectrochimica Acta Part A: Molecular and Biomolecular Spectroscopy*, **192**, 343, (2018)